High-resolution gas-phase photoelectron spectra using synchrotron radiation: Xe $4d$ linewidths and the $4d_{5/2}$:$4d_{3/2}$ branching ratio

B. W. Yates, K. H. Tan, L. L. Coatsworth, and G. M. Bancroft*
Department of Chemistry and Centre for Chemical Physics, University of Western Ontario, London, Ontario, Canada N6A 5B7 and Canadian Synchrotron Radiation Facility, Synchrotron Radiation Center, University of Wisconsin, Stoughton, Wisconsin 53589
(Received 26 July 1984)

The performance of our new gas-phase photoelectron spectrometer and the Canadian Synchrotron Radiation Facility beamline at the Synchrotron Radiation Center (Stoughton, Wisconsin) is demonstrated with use of Xe $4d$ photoelectron spectra. The beamline employs a Grasshopper monochromator with a 1° grazing angle on the M1 mirror, and the Leybold-Heraeus combined lens-analyzer system is mounted at the magic angle to eliminate polarization and β effects. Both the photon and electron resolutions are very close to theoretical, and we have obtained Xe $4d_{5/2}$ spectra with total widths as small as 0.262 eV at 94 eV photon energies. We have measured accurately and computer fitted the Xe $4d_{5/2}$:$4d_{3/2}$ branching ratio from 74 to 150 eV photon energies. There is good qualitative agreement between our measured values and the latest theoretical relativistic random-phase-approximation values. Possible reasons for quantitative differences between theory and experiment are discussed.

INTRODUCTION

In the last seven years, several gas-phase photoelectron measurements using synchrotron radiation[1-3] and line sources[4] have shown that the Xe $4d_{5/2}$:$4d_{3/2}$ branching ratio (BR) varies greatly from the statistical 1.5:1 between 70 and 200 eV photon energies. A very recent Auger study,[5] also demonstrates that the I_{N_5OO}/I_{N_4OO} Auger intensity ratio agrees semiquantitatively with the corresponding photoelectron branching ratios. Several theoretical calculations of the preceding branching ratios have been performed,[6-9] ranging from the single-particle Dirac-Fock (DF) calculations[6] to the relativistic random-phase approximation (RRPA) calculations[7,9] with some electron correlation.

Despite all previous work, there is still not quantitative agreement between theory and experiment in this relatively simple system. The agreement between the various experimental branching ratios, both at individual photon energies and for the overall trends with photon energy, is not particularly good for three reasons. First, the rather low intensity of the spectra[1-4] result in quoted standard deviations of ≥ 0.07 for most measurements. Second, it appears that strongly overlapping *NOO* Auger peaks below photon energies of 110 eV were not quantitatively accounted for. The Auger contribution can often be quite significant, as demonstrated recently by Riedel *et al.* for the valence-band $3p$ states in cleaved Si(111).[10] Third, some of the measurements were not made at the magic angle of 54.7°, causing the branching ratio to have a β dependence.[4] Even when the Auger and β problems are not important (for example, for magic angle measurements at 94 eV photon energies), the measured BR varied from 1.58 (Ref. 1) to 1.42 (Ref. 2).

The theoretical BR curves are also rather sensitive to the theoretical approximations (e.g., coupling and core relaxation effects); and the quality of the previous experimental data, although in qualitative agreement with the RRPA theoretical curve, is not good enough for quantitative comparison.

In this paper, we demonstrate the performance of our new beamline [the Canadian Synchrotron Radiation Facility (CSRF) at the Synchrotron Radiation Center, Stoughton] and photoelectron spectrometer by measuring carefully the Xe $4d_{5/2}$:$4d_{3/2}$ branching ratio at the magic angle from 74 to 150 eV photon energies; and by recording some high-resolution Xe $4d$ spectra [full width at half maximum (FWHM) for $4d_{5/2}=0.262$ eV]. We have corrected quantitatively for the *NOO* Auger peaks, and our standard deviations on the branching ratios are ≤ 0.04 for most photon energies. Hopefully, our measurements will lead to further theoretical calculations with coupling to more channels as suggested by Johnson and Radojević.[7]

EXPERIMENTAL

The Canadian Synchrotron Radiation Facility is a Canadian national facility owned by NRC (Canada) and designed for the Aladdin storage ring presently under construction. The CSRF is presently mounted on port 4 of the Tantalus storage ring. The beamline employs Aladdin optics, and is centered around a Mark IV Grasshopper monochromator[11,12] with a 1° grazing angle on the $M1$ mirror to enhance the high energy throughput. In the present study, a 900 lines/mm original ruled grating from Hyperfine Inc. was used. The second-order intensity was less than 3% of the first order with this grating. The intensity versus energy spectrum, as monitored with a Au diode, is very similar qualitatively to that reported in our previous paper[11]—the intensity peaks at 100 eV and drops

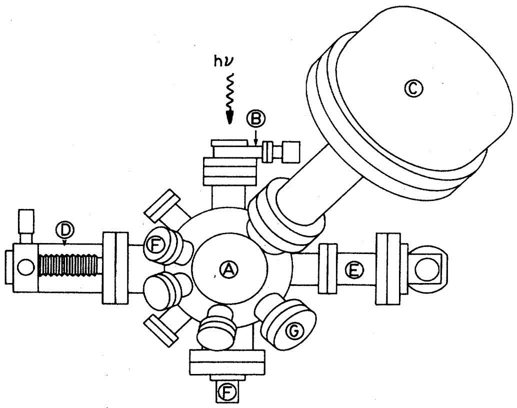

FIG. 1. Schematic diagram (top view) of the photoelectron spectrometer: *A*, sample ball; *B*, gate valve; *C*, Leybold-Heraeus combined electron lens and analyzer system; *D*, *X*-*Y*-*Z* manipulator for gas probe; *E*, CTI cryopump gas trap; F, antimagnetic view ports, and *G*, nude ionization gauge.

quite sharply at higher energies, mainly due to the decrease in synchrotron radiation intensity from this low-energy storage ring. The overall monochromator resolution is very close to the theoretical 0.06 Å for 10-μm entrance and exit slits (*vide infra*). The diverging beam from the exit slit is refocused to the sample chamber (Fig. 1,*A*) through a two-stage differential pumping system, and a high-vacuum gate valve (Fig. 1,*B*) with a rectangular glass light guide (1 mm$\times$10 mm$\times$190 mm long) supported by a graphite-coated Cu tube. This light guide results in about 5 orders of magnitude differential pumping, and the entire beamline (including both differential pumping chambers) is at a pressure of less than 2×10^{-10} Torr with a pressure in the sample chamber of $1-2\times10^{-5}$ Torr.

The sample chamber and combined lens-analyzer system were purchased from Leybold-Heraeus. The 126-mm radius spherical sample chamber is magnetically shielded (<20 mG throughout) and is pumped from below with a 500 1/s Balzers turbopump. The Leybold LHS-11 combined lens-analyzer system (Fig. 1,*C*) is mounted at the magic angle ($\alpha=\beta'=\gamma=54.7°$) so that electron intensities are independent of β and the polarization of the incident radiation.[13,14] There is additional pumping on the lens (not shown) from a 110 1/s Balzers turbopump. The gas probe is mounted on an *X*-*Y*-*Z* manipulator (Fig. 1,*D*), and gas is introduced through a stainless-steel multicapillary array with $\simeq$0.02-mm-diam holes. The gas backing pressure is controlled by a Varian Associates leak valve and measured by a MKS Inc. capacitance manometer. The gas jet is directed onto a CTI-21 cold head at 15 K (Fig. 1,*E*). With the multicapillary array, we operate at a backing pressure of 10–12 Torr which results in a ball pressure of $(1-2)\times10^{-5}$ Torr. The pressure in the interaction region of $\simeq10^{-4}$ Torr is low enough to avoid scattering cross-section problems at low kinetic energies. A channeltron detector is linked to a specially designed amplifier-discriminator counter unit and interfaced with a Digital Equipment Corporation PDP-11/23 microcomputer which controls the spectrometer using specially written data acquisition software.

For the branching-ratio studies, at least two Xe 4*d* spectra were recorded every 2 eV from 74 to 150 eV photon energies using a 50-eV analyzer pass energy. The monochromator resolution ranged from 200-μm slits ($\Delta\lambda=1.2$ Å resolution) below 130 eV photon energy to 150-μm slits ($\Delta\lambda=0.9$-Å resolution) above this, resulting in total linewidths varying between 0.8 eV at 80 eV to 1.6 eV at 150 eV. Depending on the ring current (40–200 mA), these conditions result in count rates of several hundred counts per second for energies up to 110 eV, but only a few tens of counts per second by 150 eV. Higher resolution spectra were obtained down to 30-μm slits and 25-eV pass energies.

A spectrum was collected by rapidly multiscanning the region of interest using the PDP-11/23 microcomputer. Typical data collection times per individual scan ranged from approximately 1 to 4 min, depending on the beam current and the total number of data points in the spectrum. Each individual scan was corrected before summation for the small decrease in photon flux due to beam current decay. This was done by normalizing each channel within an individual scan to the same electron current in the storage ring.

All spectra were fitted to combination Lorentzian-Gaussian peak shapes using an iterative procedure described in a previous paper.[15] The Xe $4d_{3/2,5/2}$ peak positions were constrained to differ by the high-resolution spin-orbit splitting of 1.979 ± 0.007 eV (Fig. 4 and Ref. 16). In addition to this, the linewidths and line shapes were constrained to be the same for the two spin-orbit peaks. Although a slight linewidth difference was noted at high resolution (Fig. 4) for the two peaks (see the Discussion section), this difference is negligible at the poorer resolution of 50 eV pass energy, where all the Xe 4*d* branching-ratio spectra were taken. Auger peaks were heavily constrained for <110 eV photon energies using their known positions, linewidths, line shapes, and relative areas from "clean" Auger spectra at similar photon energies.

RESULTS AND DISCUSSIONS

A typical medium resolution spectrum of the Xe 4*d* and *NOO* Auger peaks is shown in Fig. 2 for 150-μm slits ($\Delta\lambda=0.9$ Å) and 50 eV pass energy. Apart from the low kinetic energy region, the background is very low, and the linewidths of the Xe 4*d* and Auger lines are 0.83 and 0.3 eV, respectively. The Auger lines proved to be useful in determining the transmission function of the electron lens-analyzer system. Using the normalized intensities given by Werme *et al.*,[17] we confirmed that the transmission is constant over the ~25 eV kinetic energy region from ~8 eV kinetic energy (line 30) to ~34 eV kinetic energy (lines 3 and 4). This is consistent with information from Leybold,[18] which shows that the transmission should be constant to 150 eV kinetic energies for a pass energy of 50 eV. Our raw spectral data can thus be used directly without transmission corrections.

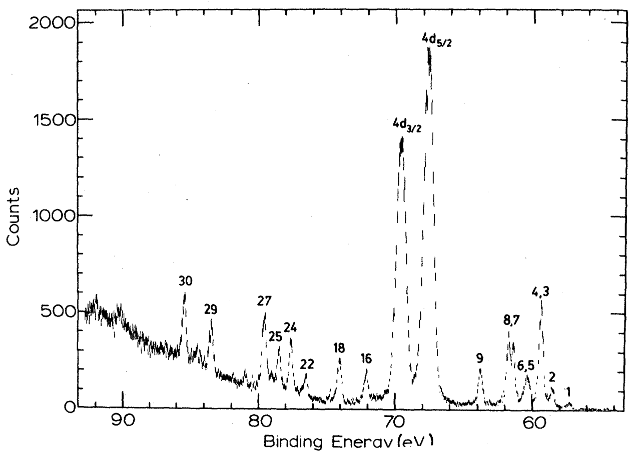

FIG. 2. Xe $4d$ and *NOO* Auger spectrum taken at 94 eV photon energies, 150-μm slits, and 50 eV pass energy. The Auger peaks are numbered according to Ref. 17.

To examine the overall beamline and photoelectron resolutions in more detail, we obtained the Xe $4d_{5/2}$ linewidths at 50-μm slits and different pass energies (Fig. 3), and recorded a Xe $4d$ spectrum at 30-μm slits and 25 eV pass energy (Fig. 4). As expected, the FWHM of the $4d_{5/2}$ line decreases as the pass energy decreases. The three data points were fit by least squares to a straight line, and extrapolation to zero pass energy yields the photon plus lifetime resolution of 0.235 eV. This value, while probably a lower limit because of the linear extrapolation, is in surprisingly good agreement with the theoretical photon plus lifetime resolution with a 900 lines/mm grating of 0.233 eV for 30-μm slits.

The Xe $4d_{5/2}$ linewidth of 0.262 ± 0.009 eV (Fig. 4) appears to be the smallest gas-phase core-level width yet observed using monochromatized sources. Comparable core-level gas-phase linewidths have been recently published by Gelius *et al.*[19] using a monochromatized Al $K\alpha$

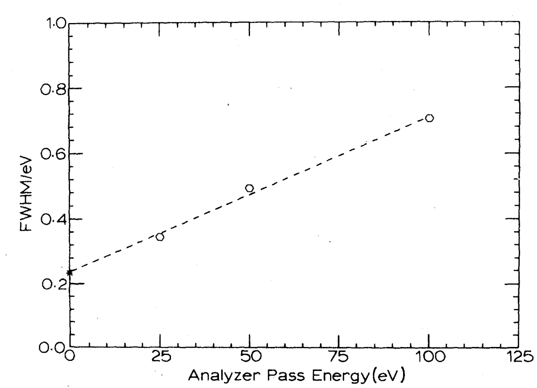

FIG. 3. Xe $4d_{5/2}$ FWHM taken at 93 eV photon energy versus pass energy for 50-μm slits. The line results from a least-squares fit to the three data points. The theoretical monochromator resolution plus the lifetime linewidth (0.233 eV) is denoted by an asterisk.

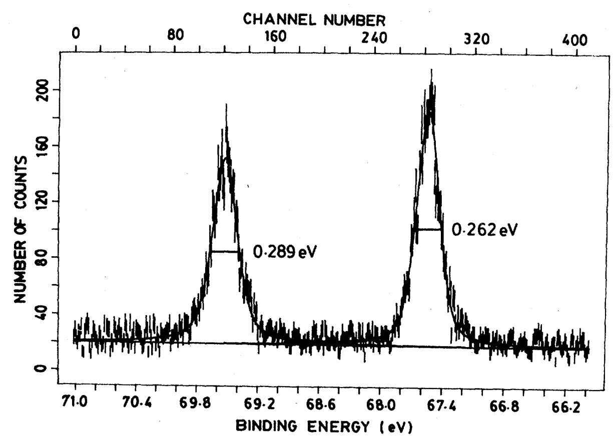

FIG. 4. Xe $4d$ spectrum taken with 94 eV photon energies with 30-μm slits and 25 eV pass energy. This spectrum took close to 3 h to accumulate. The FWHM for the two peaks are given in the figure. The measured spin orbit splitting is 1.979 ± 0.007 eV in good agreement with previous results (Ref. 16). The small Auger peaks 10—14 are all less than 1% of the intensity of the $4d$ peaks. A fit including these Auger peaks made no difference to the $4d$ linewidths.

source. Also of interest is the slightly larger linewidth of the $4d_{3/2}$ level of 0.289 ± 0.012 eV. Because the instrumental (photon plus electron) contributions to the two lines will be constant, the $4d_{3/2}$ inherent hole lifetime width must be significantly broader than the $4d_{5/2}$ lifetime width. King *et al.*[20] have measured the lifetime widths of Xe $4d$ hole states using high-resolution electron impact, and they suggest that the mean width of $4d_{5/2,3/2}$ hole states is 129 ± 8 meV, consistent with the approximate value of 100 meV evaluated by Keski-Rahkonen and Krause.[21] There is a definite hint in King's data that the $4d_{3/2}$ hole state width is larger than the $4d_{5/2}$ width by ~ 10 meV, but the errors are larger than this difference. Using the approximate expression:

$$\Gamma^2_{\text{total}} = \Gamma^2_{\text{hole state}} + \Gamma^2_{\text{experimental}} ,$$

where

$$\Gamma^2_{\text{experimental}} = \Gamma^2_{\text{photon}} + \Gamma^2_{\text{electron}} ,$$

Γ_{photon} for 30-μm slits is 0.12 eV, and $\Gamma_{\text{electron}} = 0.20$ eV for 25 eV pass energies ($E/\Delta E \simeq 125$). $\Gamma_{\text{experimental}}$ is then 0.23 eV. Using the preceding equation, the $4d_{5/2}$ and $4d_{3/2}$ hole state widths are 120 and 170 meV, respectively. Using the Voigt formula given by Keski-Rahkonen and Krause[22] to obtain more accurate values, the $4d_{5/2}$ and $4d_{3/2}$ hole state widths are still quite different but much smaller—54 and 100 meV. The errors on these numbers are ~ 20 meV.

Differences in widths of spin-orbit components have been seen recently on $4f$ levels of Hf, Ta, and W.[23,24] The larger $4f_{5/2}$ width has been attributed to an $N_6N_7O_{4,5}$ Coster-Kronig decay which reduces the lifetime of the $4f_{5/2}$ core hole state relative to the $4f_{7/2}$ core hole state. Such a mechanism cannot be responsible for our difference, however, and further theoretical work is required.

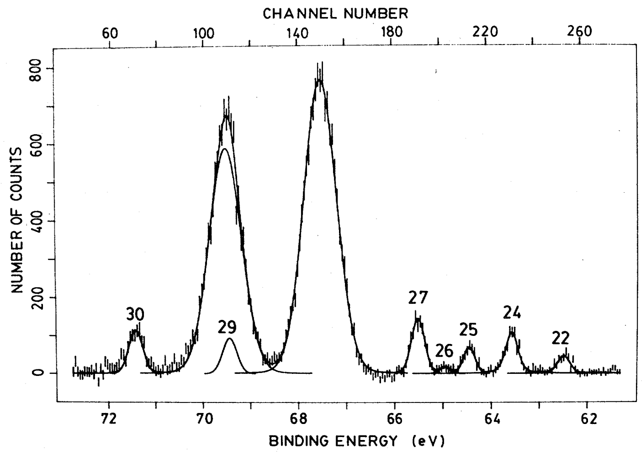

FIG. 5. Xe $4d$ spectrum taken at 80 eV photon energies, 200-μm slits, and 50 eV pass energy. Note the significant contribution of Auger peak 29 to the $4d_{3/2}$ peak. Inclusion of the weak Auger peak 28 (not shown) on the low binding-energy edge of the $4d_{5/2}$ peak, makes no significant difference to the branching ratio.

Because we can go to much smaller slit widths (10 μm) and pass energies (2.5 eV), it is apparent that we will eventually be able to obtain narrower Γ_{total} values for narrow lines such as Xe $4d$ when we obtain higher photon fluxes (e.g., with new M1 optics or on Aladdin), or higher gas pressures in the interaction region (e.g., with a gas cell).

Turning now to branching ratios, a typical spectrum of the Xe $4d$ levels with 80 eV photon energies (Fig. 5) shows the problem of obtaining accurate BR values when there are overlapping Auger lines. If the Xe $4d_{5/2,3/2}$ lines are fitted without including Auger peak 29, a BR of 1.13 results; when the Auger peak is properly fitted, a BR of 1.30 results. Differences of at least 0.2 can arise with small shifts in Auger peaks relative to the $4d$ peaks. Correction without computer fitting is thus very difficult indeed.

The standard deviations from the computer fits on the BR values for most of our individual spectra such as shown in Fig. 5 are ± 0.02 to ± 0.05. Are these errors realistic? Using the statistical treatment outlined in Topping and Clark *et al.*[25,26] the two independent expressions for the standard error of the mean for the branching ratios can be evaluated:

$$\alpha_i^2 = \left[\sum_{j=1}^{n} \frac{1}{S_j^2} \right]^{-1}$$

and

$$\alpha_e^2 = \left[\sum_{j=1}^{n} \frac{(X_j - \bar{X})^2}{S_j^2} \right] \left[(n-1) \sum_{j=1}^{n} \frac{1}{S_i^2} \right]^{-1},$$

where α_i is a function of the internal consistency and α_e of the external consistency of the observations. S_j is the associated standard deviation for the branching ratios obtained from the computed spectra (Table I). Snedecor's F test ($F = Z^{\pm 2}$ where $Z = \alpha_e / \alpha_i$) was used to check that α_i^2 and α_e^2 could reasonably be expected to be estimates of the same variance. The weighted means α_e, α_i, and Z are given in Table I for a number of spectra at two different photon energies. In all cases, the Z values are statistically acceptable, indicating that our standard deviations are realistic and that any nonrandom effects are not influencing our spectra and the BR values.

The BR versus photon energy plot is given in Figs. 6(a) and 6(b) along with the latest theoretical RRPA results given by Cheng and Johnson,[9] done in intermediate coupling using six interacting channels ($4d_{3/2} \to p_{1/2}, p_{3/2}, f_{5/2}$; $4d_{5/2} \to p_{3/2}, f_{5/2}, f_{7/2}$). Our results are in good qualitative agreement with the RRPA results, and not in agreement with the earlier Dirac-Fock (DF) results (*jj* coupling) which are far too large above 100 eV.[6] Most of our BR values are significantly smaller than those obtained earlier (see Fig. 2, Ref. 4), many of which were reported to be very close to the statistical ratio of 1.5. From 98 to 146 eV our BR falls very slowly and monotonically [Fig. 6(a)]. The agreement with RRPA in this region is rather good, although it should be noted that the experimental data are consistently a little lower than the theoretical curve. Since the Dirac-Hartree-Fock (DHF) results which include part of the RRPA correlations are larger than the RRPA results in this region,[7] we suspect that agreement would be improved by including the coupling and correlation of the $4d$ shell with the adjacent $4s$, $4p$, $5s$, and $5p$ subshells. Including just the $5s$ and $5p$ subshells increases the number of channels from six to thirteen.

To within the quoted errors, good agreement also occurs for the lower photon energies of 74, 75, 76, and 78 eV [Fig. 6(b)]. The largest deviations occur around the minimum region between 80 and 86 eV where correlation effects are strongest. The experimental minimum occurs

TABLE I. Reproducibility of branching ratio (BR).

Photon energy (eV)	BR	(S)	$\overline{\text{BR}}$	α_i	α_e	Z
120	1.323	(0.045)				
	1.293	(0.024)	1.293	0.014	0.007	0.50
	1.288	(0.021)				
110	1.338	(0.031)	1.326	0.015	0.007	0.47
	1.334	(0.035)				
	1.308	(0.027)				
	1.333	(0.032)				

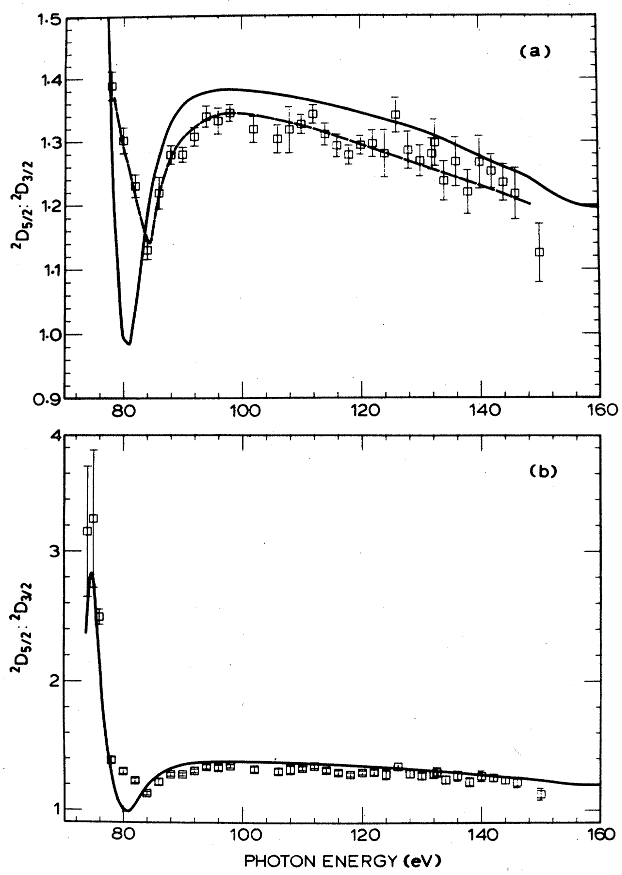

FIG. 6. Xe $4d_{5/2}$:$4d_{3/2}$ BR as a function of photon energy (a) from 78 to 150 eV; (b) from 74 to 150 eV. The error bars given are the larger of α_i or α_e. The dashed line is a visual fit to the experimental data; the solid line is the latest RRPA theoretical results of Cheng and Johnson (Ref. 9).

at 84 eV photon energy, 3 eV higher than that predicted by the RRPA calculations. Furthermore the experimental minimum region is not as deep or as pronounced as in the RRPA calculation. Including coupling with other subshells might partially account for some of these differences.

Although electron correlations are accurately accounted for by the random-phase approximation, strong correlation between the low-energy photoelectron near threshold and the residual ion are not properly accounted for. Extensions have been made to the random-phase approximation (RPA) to include such "relaxation" effects at low kinetic energies, improving the agreement for atomic Ba.[27,28] Relaxation effects tend to change the total cross-section shape, magnitude, and maximum position.[27,28] As Wendin has pointed out,[27] relaxation effects can shift ionization thresholds and deform the shape of the cross section near the threshold, so that simply introducing experimental binding energies into the RPA equations can be very bad when the photoionization cross section is quite peaked near threshold. We feel, therefore, that inclusion of double excitations accounting for relaxation of the frozen core, shakeup or shakeoff, and Auger transitions is necessary in the threshold region of Xe $4d$. Hopefully these data will encourage further expanded RRPA calculations to be performed on the Xe $4d$ levels, so that the relative importance of these effects can be determined.

Finally, it is interesting to note that our BR value at 150 eV (1.125 ± 0.045) is significantly below that expected from our measured values and the theoretical curve. Southworth *et al.*[5] also obtained very low I_{N_5OO}/I_{N_4OO} Auger ratios in this region (0.96 ± 0.14 at 155 eV, and 1.09 ± 0.18 at 162 eV). Unfortunately the errors in both measurements are rather large because of the low photon intensity and small cross sections at these energies. Such a change is probably due to the onset of the $4p_{1/2}$ ionization (the binding energy is 145.51 eV),[29] which by analogy with the Kr $4p$ ionization should reach its maximum cross section at 5—10 eV above threshold.[30] This effect is very similar to the decrease noted by Wertheim[31] in the Se $3d_{5/2}$-to-$3d_{3/2}$ BR when ionizing the Se $2p_{1/2}$ level (the binary energy is 1476 eV) with Al $K\alpha$ radiation. Clearly, more accurate experimental measurements are required to confirm this effect.

ACKNOWLEDGMENTS

We would like to acknowledge the cooperative administrative assistance of Dr. N. K. Sherman (NRC), the technical assistance of I. Schmidt, the helpful advice and assistance of the staff at Baker Engineering and at the Synchrotron Radiation Center (Stoughton), especially C. G. Olson, F. C. Brown, N. Lien, and C. A. Pruett; and W. R. Johnson and K. T. Cheng for sending us their theoretical RRPA branching-ratio data. We are very grateful to the National Research Council (NRC) of Canada, the Natural Sciences and Engineering Research Council (NSERC) of Canada, and the University of Western Ontario for financial support.

*To whom correspondence should be addressed.

[1]S. P. Shannon, K. Codling, and J. B. West, J. Phys. B **10**, 825 (1977).

[2]F. Wuilleumier, M. Y. Adam, N. Sandner, V. Schmidt, W. Mehlhorn, and J. P. Desclaux, *Extended Abstracts, Proceedings of the 5th International Conference on VUV Radiation, Montpelier, 1977,* edited by M. C. Castex, M. Pouey, and N. Pouey (CNRS, Paris, 1977), p. 14.

[3]M. Y. Adam, F. Wuilleumier, S. Krummacher, N. Sandner, V. Schmidt, and W. Mehlhorn, J. Electron Spectros. Relat. Phenom. **15**, 211 (1979).

[4]M. S. Banna, M. O. Krause, and F. Wuilleumier, J. Phys. B **12**, L125 (1979).

[5]S. Southworth, V. Becker, C. M. Truesdale, P. H. Kobrin, D. W. Lindle, S. Owaki, and D. A. Shirley, Phys. Rev. A **28**, 261 (1983).

[6]W. Ong and S. T. Manson, Bull. Am. Soc. **23**, 564 (1978).
[7]W. R. Johnson and V. Radojević, J. Phys. B **11**, L773 (1978).
[8]J. P. Desclaux (unpublished), quoted in Refs. 2 and 7.
[9]K. T. Cheng and W. R. Johnson, Phys. Rev. A **28**, 2830 (1983).
[10]R. A. Riedel, M. Turowski, and G. Margaritondo, Phys. Rev. Lett. **52**, 1568 (1984).
[11]K. H. Tan, G. M. Bancroft, L. L. Coatsworth, and B. W. Yates, Can. J. Phys. **60**, 131 (1982).
[12]F. C. Brown, R. Z. Bachrach, and N. Lien, Nucl. Instrum. Methods **152**, 73 (1978).
[13]J. A. R. Samson, J. Opt. Soc. Am. **59**, 356 (1969).
[14]J. A. R. Samson, Philos. Trans. R. Soc. London **A268**, 141 (1970).
[15]G. M. Bancroft, I. Adams, L. L. Coatsworth, C. D. Bennewitz, J. D. Brown, and W. D. Westwood, Anal. Chem. **47**, 536 (1975).
[16]G. M. Bancroft, P. A. Malmquist, S. Svensson, E. Basilier, U. Gelius, and K. Siegbahn, Inorg. Chem. **17**, 1595 (1978), and references therein.
[17]L. O. Werme, T. Bergmark, and K. Siegbahn, Phys. Scr. **6**, 141 (1972).
[18]M. Wilmers (private communication).
[19]U. Gelius, L. Asplund, E. Basilier, S. Hedman, K. Helenelund, and K. Siegbahn, Nucl. Instrum. Methods **229**, 85 (1984).
[20]G. C. King, M. Tronc, F. H. Read, and R. O. Bradford, J. Phys. B **10**, 2479 (1977).
[21]O. Keski-Rahkonen and M. O. Krause, At. Data Nucl. Data Tables **14**, 139 (1974).
[22]O. Keski-Rahkonen and M. O. Krause, Phys. Rev. A **15**, 959 (1977).
[23]J. F. Vander Veen, F. J. Himpsel, and D. E. Eastman, Phys. Rev. B **25**, 7388 (1982).
[24]R. Nyholm and J. Schmidt-May, J. Phys. C **17**, L113 (1984).
[25]J. Topping, *Errors of Observation and Their Treatment* (The Institute of Physics and Physical Society, London, 1961).
[26]M. G. Clark, G. M. Bancroft, and A. J. Stone, J. Chem. Phys. **47**, 4250 (1967).
[27]G. Wendin, *Photoionization and other Probes of Many-Electron Interactions*, edited by F. J. Wuilleumier (Plenum, New York, 1976), p. 74.
[28]S. L. Carter and H. P. Kelly, J. Phys. B **11**, 2467 (1978).
[29]U. Gelius, J. Electron Spectros. Relat. Phenom. **5**, 985 (1974).
[30]K. N. Huang, W. R. Johnson, and K. T. Cheng, At. Data Nucl. Data Tables, **26**, 33 (1981).
[31]G. K. Wertheim, J. Electron Spectros. Relat. Phenom. **33**, 79 (1984).